

ENERGY DISTRIBUTION OF HEATING PROCESSES IN THE QUIET SOLAR CORONA

SÄM KRUCKER^{1,2} AND ARNOLD O. BENZ¹

Received 1998 April 10; accepted 1998 May 7; published 1998 June 26

ABSTRACT

We have determined the variations in the emission measure of the solar corona using EUV Imaging Telescope/*Solar and Heliospheric Observatory* observations of iron lines in a quiet region of the Sun. The emission measure is found to vary significantly in at least 85% of all the pixels within 42 minutes. The variations are interpreted as heating events that bring chromospheric material above the one million degree threshold of the observed lines and that cool the coronal plasma below that limit. A method to assess heating events has been developed. The thermal energy input by such microflares is calculated from the observed increases in emission measure and the derived temperature. Heating events have been found in the range from 8×10^{24} to 1.6×10^{26} ergs. The energy input by $\geq 3 \sigma$ events of the emission measure increase the amounts to about 16% of the average radiated power of the coronal plasma in the quiet corona. The frequency distribution of microflares is an approximate power law of the form $f(E) = f_0 E^{-\delta}$, with a power-law index δ between 2.3 and 2.6. Since the low-energy cutoff is due to sensitivity limitations and the power-law index is steeper than 2, these observations demonstrate the possibility that microflares dominate the energy input into the quiet corona. The observed power law would have to continue to about 3×10^{23} ergs in order to match the observed minimum heating requirement.

Subject headings: Sun: activity — Sun: corona — Sun: flares — Sun: X-rays, gamma rays

1. INTRODUCTION

The quiet corona is at a surprisingly constant temperature (see, e.g., Brosius et al. 1997 and references therein). On the other hand, it has been proposed that small flares (microflares or nanoflares) heat the corona (see reviews in Ulmschneider, Rosner, & Priest 1991 and Zirker 1993). Evidence has been presented showing that the emerging magnetic flux may provide enough energy to heat the corona by the release of magnetic energy (see, e.g., Schrijver et al. 1997). Furthermore, a large number of brightenings in the corona/chromosphere transition region have been reported (Lites & Hansen 1977; Brueckner & Bartoe 1983; Porter et al. 1987; Harrison 1997; review by Dere 1994). Here we investigate the energy input that is actually observed to arrive in the corona.

Small, soft X-ray microflares above the network of the quiet Sun have been discovered by Krucker et al. (1997a). The brightenings are caused mostly by an increase of the coronal emission measure (Krucker et al. 1997a; Krucker, Benz, & Delaboudinière 1997b). The observed coronal temperature increases only slightly during these X-ray events. Thus, the increase in the coronal emission measure (square of density times volume) was interpreted by these authors as evaporation events similar to regular flares in active regions. This was supported by the observation of associated radio emissions, some of which peaked before the soft X-rays and were polarized (and thus were possibly of nonthermal origin). Except for the low temperature, these properties are typical for regular flares, supporting the interpretation of soft X-ray brightenings as microflares. The energy input can be readily estimated from the thermal energy of the newly heated material injected into the corona.

The possibility of creating the corona by the chromospheric evaporation of microflares is a variety of the microflare heating model. An obvious requirement is that the energy input observed in the emission measure enhancements be sufficient

enough to balance the radiation loss of the corona. The problem is identical to the analysis of the energy input by regular flares. The energy input has been evaluated by integrating in energy the rate of flare energy release, $f(E)$, observed at the energy E per unit area. Thus, the flare input power is

$$P = \int_{E_{\min}}^{E_{\max}} E f(E) dE \quad (\text{ergs s}^{-1} \text{ cm}^{-2}). \quad (1)$$

The minimum energy E_{\min} is usually set by instrumental limits, and the maximum energy E_{\max} by some high-energy cutoff or the largest flare that occurred in the observing period. If the distribution of the thermal energy is a power law, $f(E) = f_0 E^{-\delta}$, the integral in equation (1) behaves differently, depending on δ being larger or smaller than 2. If $\delta > 2$ and $E_{\min} \ll E_{\max}$, the result is

$$P \approx \frac{f_0}{\delta - 2} \frac{1}{E_{\min}^{\delta-2}}. \quad (2)$$

It is dominated by the low-energy part of the energy range (Hudson 1991). The reverse holds if $\delta < 2$.

For regular flares (generally located in *active regions*), the observations have mostly been analyzed by peak flux or peak count rate measurements. The results are power-law distributions with indices δ around 1.8 (Datlowe, Elcan, & Hudson 1974; Lin et al. 1984; Dennis 1985; summarized by Crosby, Aschwanden, & Dennis 1993). The latter authors also present a substantial investigation of the total energy in the flare electrons observed in hard X-ray bremsstrahlung, finding $\delta = 1.53 \pm 0.02$.

Soft X-ray peak fluxes of regular flares have a power-law index between 1.84 (Hudson, Peterson, & Schwartz 1969) and 1.75 (Drake 1971). The latter author reports an exponent of the fluence (time-integrated flux, proportional to the total radiated flare energy) of 1.44. Shimizu (1995) finds a power-law index between 1.5 and 1.6 for flare thermal energy inputs larger

¹ Institute of Astronomy, ETH-Zentrum, CH-8092 Zürich, Switzerland.

² Space Sciences Laboratory, University of California at Berkeley, Berkeley, CA 94720-3411.

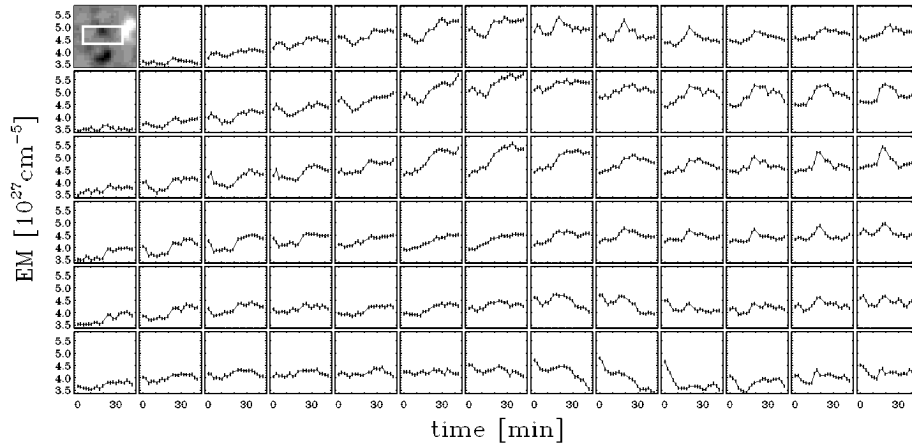


FIG. 1.—Coronal emission measure vs. time for single, adjacent pixels, each having a size of $2''.6 \times 2''.6$. A typical sample of only 77 out of the total number of 23,800 pixels is shown. The error bars are conservative upper limits, as explained in the text. In the upper left-hand corner, the displayed area is marked on a magnetogram (*SOHO*/MDI data).

than 10^{27} ergs, as determined from soft X-ray brightenings in active regions. He estimates that the energy supplied by these small flares is at most 20% of the required amount to heat the corona in active regions. The flat distribution ($\delta < 2$) suggests that the flares below the sensitivity limit cannot be responsible for the rest of the energy input.

If flares heat the corona, they must not only be smaller (microflares) but more numerous. Thus, their power-law index must exceed 2. Vlahos et al. (1995) have simulated the coronal energy release by avalanche models. Their anisotropic version predicts small flares having a power-law index of 3.5.

Here the question of coronal heating in *quiet regions* is investigated using sensitive, high-temperature iron lines in EUV that originate directly from the corona. They allow the derivation of the coronal emission measure with less noise than previous soft X-ray observations.

2. OBSERVATIONS AND ANALYSIS

The observations were made with the EUV Imaging Telescope (EIT) on board the *Solar and Heliospheric Observatory (SOHO)* satellite (Delaboudinière et al. 1995). The normal-incident, multilayered mirror instrument imaged a $7' \times 7'$ area of the quiet Sun in the center of the solar disk. The spatial and temporal resolutions were $2''.6$ and 127.8 s, respectively. Two wavelength bands at 171 and 195 Å have been measured alternatively. They include Fe IX–X and Fe XII lines, respectively, yielding diagnostics for plasma in the temperature range of $(1.1\text{--}1.9) \times 10^6$ K. Using the two bands, a formal emission measure and a formal temperature have been determined for each pixel and at each time using standard EIT software. The photon counting noise introduces a mean statistical error of 2% in the derived values of the emission measure. However, the systematic errors introduced by the uncertainty in inhomogeneity, in the chemical abundances, in the atomic physics, and in the filling factor are probably larger but unknown. The derived parameters can be interpreted as weighted averages over the sensitive range of temperatures in the pixel area and must be taken as formal values, quantitatively related to the physical reality in a complex way. Nevertheless, they are assumed here to be good enough proxies for our purposes.

Figure 1 shows the change of the coronal emission measure

in individual pixels during the observing time of 42 minutes. Pixels above the magnetic network boundary and, in particular, above the bipolar spot (cf. insert) generally have an elevated level. Significant fluctuations are present in practically every pixel. The event seen in the middle of the right edge is one of the 23 most intense events analyzed in detail by Benz & Krucker (1998). Figure 1 indicates that the definition of single “events” is critical. The effects of several assumptions have been investigated and are described in §§ 2.1 and 2.2.

2.1. Amplitude Parameters

The emission measure time series of each pixel has been searched for local peaks. A peak is marked if it exceeds the emission measures of the pixel at the previous and following time steps.

The standard deviation σ has been determined from the distribution of fluctuations in the emission measure by Benz & Krucker (1998), yielding an effective number that includes photon noise and other sources. Here a more conservative value, derived from instrument calibrations, is used, which is 20% larger (T. D. Tarbell 1998, private communication). This assumption does not affect the final result and can be considered a part of the free parameter a defined below.

The minimum value represents the background. It is defined in two ways. In version A, it is the minimum value between the peak and the previously accepted peak or the start of the time series. In version B, it is the absolute minimum of the pixel’s time series.

The peak is only considered for further analysis if it exceeds the minimum value by some factor a of the standard deviation, σ . The value a is a free parameter to be chosen later.

2.2. Spatial Parameters and Energy

The network flares presented by Krucker et al. (1997a, 1997b) comprise several tens of square arcseconds. Therefore, events seen in 1 pixel (local peaks) have to be checked for simultaneous events in adjacent pixels. Simultaneous local peaks in adjacent pixels are considered as one event. Only the immediately neighboring pixels north, south, east, and west of a given pixel have been checked. In version 1, local peaks are

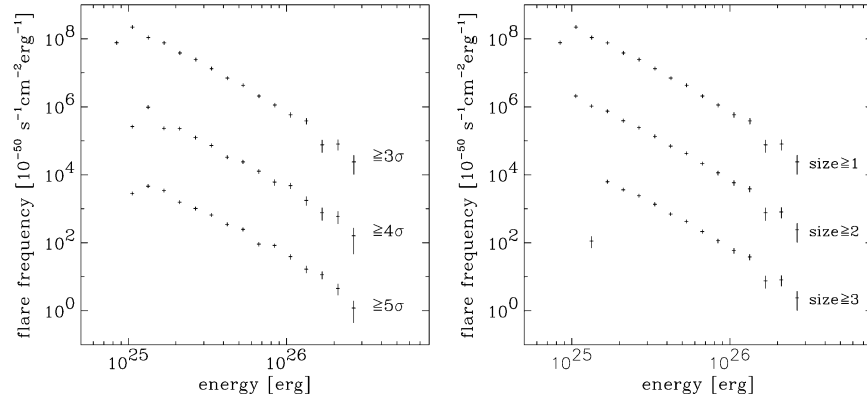


FIG. 2.—(a) The number of flares per unit time, area, and energy is shown vs. the thermal flare energy. The error bars (vertical) indicate the statistical error due to the number counting. Three versions are displayed with minimum peak enhancement of the emission measure by 3 σ , 4 σ , and 5 σ . They are subsequently offset by a factor of 100. The power-law approximation to the flat part of the log-log distribution of ≥ 3 σ events is $f(E) = f_0 E^{-2.59}$. (b) Similar to (a), but for ≥ 3 σ events. In addition, a requirement on the minimum event area has been introduced. Three versions are displayed with a minimum event area of 1 [same as (a)], 2, and 3 pixels. They are subsequently offset by a factor of 100.

combined if they occur simultaneously or one time step (2 minutes) earlier or later. In version 2, adjacent pixels are only combined if they peak in the same time bin.

Finally, the enhancements in the emission measure are converted into the thermal energy content. According to our interpretation, as evaporation events, the temperature increases from a chromospheric to a coronal value. Thus, the thermal energy input amounts to about $3\Delta N k_B T$, where T is the final temperature of the newly heated plasma and $2\Delta N$ is the total number of particles (electrons and ions). With $\Delta \mathcal{M}$ being the observed increase in the emission measure in the area A of the enhancement, the thermal energy input is

$$E = 3k_B T \sqrt{\Delta \mathcal{M} A q h} \text{ (ergs)}. \quad (3)$$

The height h and filling factor q of the newly heated material are model parameters. Benz & Krucker (1998) have estimated them, in an event, to be $qh \approx 5000$ km. This value will be used in our numerical estimates. If the actual value is smaller, the thermal energy is reduced by the square root of the factor qh_{5000} and vice versa. The thermal energy input may be compared with the radiative and convective energy losses of the newly heated plasma. For X-ray brightenings in active regions, Shimizu (1995) has found higher values for these losses than for the thermal energy input by a factor of about 5. However, the assumptions that enter the estimate, in particular on the convective loss, are even more model dependent. It is nevertheless important to note that the thermal energy input as derived in equation (3) is a lower limit to the total energy input.

The temperature in equation (3) has been derived for each pixel and time step. The formal value is probably an underestimate for the newly heated material since it is the pixel average weighted over the sensitive temperature range. The highest temperature derived in the field of view is 1.5×10^6 K. Thus, the plasma having a temperature above the sensitive range seems to be a small fraction and will be neglected in the following.

The choice of parameters and of version has been guided by the experience of network flares (Krucker et al. 1997a), as well as the detailed evaluation of the 23 largest events in this same set of observations by Benz & Krucker (1998). The largest areas of these events reach 16 pixels, about 100 arcsec^2 .

Version 1, which allows slightly nonsimultaneous pixels to be combined into one event, produces unrealistically large event areas. At a significance of 1 σ , 90% of all local peaks are part of events that exceed 16 pixels. For ≥ 5 σ events, this number is still 20%. Such sizes exceed the area of the most intense events. Furthermore, version 1 tends to produce weak events with longer duration than these most intense events. Therefore, the comparison with intense events suggests that version 1 combines unrelated events effectively. Version 2 timing, which allows only simultaneous pixels to be combined, also occasionally produces event areas larger than 16 pixels. For ≥ 2 σ , they amount to less than a few percent of the local peaks.

Version B, which uses the lower minimum value, produces relatively large energies, some exceeding the numbers for the published network flares. The main effect on the flare distribution of version B compared with version A is a shift to higher energies without changing significantly the power-law index. Version A is thus used in the following way.

3. RESULTS AND DISCUSSION

Plausibility arguments and a comparison with well-defined, intense network flares studied previously favor the version A2 method described above. It combines only simultaneously peaking pixels and measures the emission measure enhancements from the preceding minimum. Using pixels with variations above 0 σ , 3 σ , 4 σ , and 5 σ , version A2 yields 26,619, 11,150, 5302, and 2598 events in the field of view ($7' \times 7'$) and during the observing time of 42 minutes, respectively. The ≥ 0 σ number, comprising all enhancements, includes events that are due to noise.

Figure 2a displays the flare distribution for various lower limits of the peak using the method in version A2. The events range from 8×10^{24} to 2.8×10^{26} ergs. A low-energy turnover is apparent at 10^{25} ergs, which increases with the limit on σ . It corresponds to the limiting energy set by a σ and is therefore due to the limited sensitivity. The distributions presented in Figure 2a are approximate power laws that span over more than a decade. The power-law index was determined by a regression to the straight part of the distribution in the log-log representation. For a 3 σ and 4 σ limit, a power-law index of 2.59 and 2.54 is found, respectively. It decreases to 2.31 for

events $\geq 6\sigma$. At the 2σ lower limit and below, the power-law form of the distribution disappears.

Figure 2*b* shows the flare distribution with an additional requirement concerning the event area. It is a test on the effect of combining adjacent, simultaneous events. If a minimum area is required and is increased from 1 to 3 pixels, the low-energy cutoff shifts from 1.0×10^{25} to 1.6×10^{25} ergs. This indicates that the smallest events have an area of only 1 or 2 pixels. The power-law index, however, remains 2.52 ± 0.02 for minimum sizes up to 3 pixels. It decreases to 2.34 for event sizes ≥ 4 pixels. The robustness of the index on the minimum event area is reassuring.

It is thus concluded that the power-law index of the energy input of microflares in the quiet corona is between 2.3 and 2.6. The energy input by all microflares observed above a given threshold can be obtained by integrating the values displayed in Figure 2*a*. The thermal energy input by the microflares has been divided by the total observing time and the area of the field of view. The result is the thermal input power per unit area and amounts to $P = 7.1 \times 10^4$ ergs $s^{-1} cm^{-2}$ for events $\geq 3\sigma$.

The average total radiation loss of the corona in the field of view can also be calculated for each pixel and time step using the formal emission measure and average temperature. The SPEX software package (Kaastra, Mewe, & Nieuwenhuijzen 1996) has been used, assuming collisional ionization equilibrium and photospheric abundances. The total average radiative output (full sphere) divided by the area is found to be $(4.5 \pm 1.1) \times 10^5$ ergs $s^{-1} cm^{-2}$. It includes all radiation losses in the continuum and the lines from UV to X-rays.

Thus, the observed $\geq 3\sigma$ events in the coronal emission measure enhancements constitute about 16% of the required energy to create the quiet corona and radiate the observed emission. The value is a lower limit to the total energy input but is also model dependent.

4. CONCLUSIONS

Enhancements in coronal emission measure have been observed and interpreted as heating events by microflares. The enhancements investigated here are impulsive, and they are limited by the observations to scales between 2 and 42 minutes. These timescales are comparable to the durations of regular soft X-ray flares in active regions and contain the peak of their distribution (Drake 1971).

The thermal energy content of microflares has been determined at the peak of the emission measure enhancement. At low energies, about 10^{25} ergs, the distribution is cut by limited sensitivity. The energy distribution of the enhancements is an approximate power law with an index between 2.3 and 2.6. For such a power-law distribution with an index above 2, the derived thermal energy input is limited by the low-energy cutoff and is a lower limit.

The observed enhancements in emission measure ($\geq 3\sigma$) constitute a considerable energy input into the corona. However, the observation of a relatively steep power-law slope is more important than the derived fraction of the microflare energy input. Due to this steep index of more than 2, it cannot be excluded that enhancements smaller than the sensitivity limit of these observations constitute the major energy input. Equation (2) indicates that the observed power law would have to continue to about 3×10^{23} ergs, comprising about 28,000 microflares per second on the whole Sun, to match the observed radiation loss.

We thank the EIT team for their excellent work (in particular, J.-P. Delaboudinière and B. J. Thompson) and M. J. Aschwanden and M. Güdel for a critical reading of the manuscript. *SOHO* is a joint project between the European Space Agency and NASA. EIT was funded by CNES, NASA, and the Belgian SPPS. The work at ETH Zürich is financially supported by the Swiss National Science Foundation (grant 20-046656.96).

REFERENCES

- Benz, A. O., & Krucker, S. 1998, *Sol. Phys.*, submitted
 Brosius, J. W., Davila, J. M., Thomas, R. J., Saba, J. I. R., Hara, H., & Monsignori-Fossi, B. C. 1997, *ApJ*, 477, 969
 Brueckner, G. E., & Bartoe, J.-D. F. 1983, *ApJ*, 272, 329
 Crosby, N. B., Aschwanden, M. J., & Dennis, B. R. 1993, *Sol. Phys.*, 143, 275
 Datlowe, D. W., Elcan, M. J., & Hudson, H. S. 1974, *Sol. Phys.*, 39, 155
 Delaboudinière, J.-P., et al. 1995, *Sol. Phys.*, 162, 291
 Dennis, B. R. 1985, *Sol. Phys.*, 100, 489
 Dere, K. P. 1994, *Adv. Space Res.*, 14(4), 13
 Drake, J. F. 1971, *Sol. Phys.*, 16, 152
 Harrison, R. A. 1997, *Sol. Phys.*, 175, 467
 Hudson, H. S. 1991, *Sol. Phys.*, 133, 357
 Hudson, H. S., Peterson, L. E., & Schwartz, D. A. 1969, *ApJ*, 157, 389
 Kaastra, J. S., Mewe, R., & Nieuwenhuijzen, H. 1996, in *UV and X-Ray Spectroscopy of Astrophysical and Laboratory Plasmas*, ed. K. Yamashita & T. Wanatabe (Tokyo: Universal Academy Press), 411
 Krucker, S., Benz, A. O., Acton, L. W., & Bastian, T. S. 1997a, *ApJ*, 488, 499
 Krucker, S., Benz, A. O., & Delaboudinière, J.-P. 1997b, in *Fifth SOHO Workshop, The Corona and Solar Wind Near Minimum Activity*, ed. O. Kjeldseth-Moe (ESA SP-404; Noordwijk: ESA), 465
 Lin, R. P., Schwartz, R. A., Kane, S. R., Pelling, R. M., & Hurley, K. C. 1984, *ApJ*, 283, 421
 Lites, B., & Hansen, E. R. 1977, *Sol. Phys.*, 55, 347
 Porter, J. G., et al. 1987, *ApJ*, 323, 380
 Schrijver, C. J., Title, A. M., van Ballegoijen, R. A., Hagenaar, H. J., & Shine, R. A. 1997, *ApJ*, 487, 424
 Shimizu, T. 1995, *PASJ*, 47, 251
 Ulmschneider, P., Rosner, R., & Priest, E. R., eds. 1991, *Mechanisms of Chromospheric and Coronal Heating* (Berlin: Springer)
 Vlahos, L., Georgoulis, M., Kluiving, R., & Paschos, P. 1995, *A&A*, 299, 897
 Zirker, J. 1993, *Sol. Phys.*, 148, 43